Extracting the generalized parton distributions of protons through hard exclusive heavy meson production

Tyler Schroeder[1], Marie Boer[2]

[1]*College of William and Mary, Williamsburg, VA, U.S.A*, [2]*Virginia Polytechnic Institute and State University, Blacksburg, VA, U.S.A*

Abstract

Heavy meson production is a key tool for accessing the inner dynamics of the proton. These production reactions involve the proton Generalized Parton Distributions (GPDs), which correlate the longitudinal momenta and their transverse distribution of the proton's composite partons. The hard exclusive production of Quarkonia (J/ψ, Υ, etc.) is particularly interesting, as it accesses the gluon GPDs at the lowest order. We used ROOT to create a new flexible generator for the photoproduction, quasi- photoproduction, and electroproduction of vector mesons off a proton. The output phase space is weighted by the reaction cross-section, creating a realistic graph of event count as a function of energy. We will discuss the relevance of measuring hard exclusive production of Quarkonia, present our work on the event generator, and discuss our projections for the upcoming Electron-Ion Collider (EIC).

Keywords: Generalized Parton Distributions, Deeply Virtual Meson Production, Jefferson Lab, Electron-Ion Collider, Simulation

1. Background

1.1 Introduction

It has been a longstanding goal of particle physics to describe the inner dynamics of the proton. The first notable attempt at this was Richard Feynman's parton model,

which proposed that the proton consisted of three "valence" partons. These partons were quickly identified as quarks, which are particles that come in two families (those with electric charge $+2/3$ and those with electric charge $-1/3$) and carry one of three "color" charges (red, green, or blue). A key theoretical fact is that particles made up of quarks are only stable if their their colors "add up" to white. For example, a proton must at any time have exactly one red, green, and blue quark.[1]

2

Fig. 1. The six quarks of the Standard Model and the relevant force carriers.

However, it was soon discovered that *which* quark was red, green, or blue was not constant. Rather, two valence quarks can swap colors by exchanging a massless particle known as a *gluon*. This constant exchange of gluons inside a proton(as well as virtual gluon pairs which emerge from the vacuum) forms what is known as the proton's *gluon sea*. Gluons from this sea are able to interact with particles at high energies, either directly or by splitting into a virtual quark-antiquark pair. Thus, to fully describe the interior of a proton, one must describe both the proton's valence quarks and its gluon sea.[1]

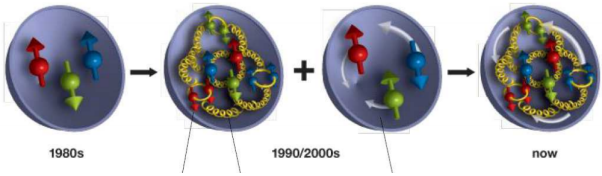

Fig. 2. The evolution of the proton model.[3]

The interplay of quarks and gluons is too complex to calculate theoretically using perturbative QCD. Instead, their distribution is described using experimentally-determined *Generalized Parton Distributions* (GPDs). GPDs are functions that relate the longitudinal (parallel) momentum of a quark or gluon to its transverse distribution inside the proton.[1]

The best way to measure GDPs is to conduct scattering reactions off the proton. At high energies, the probability amplitude for these reactions can be factored into a theoretically-calculable "hard" part, described by a differential cross section, and

an approximate "soft" part described by the GPD. An example is Timelike Compton Scattering, the scattering of a photon off a proton, which can be drawn with the "hard" part above the line and the "soft" part below:[4]

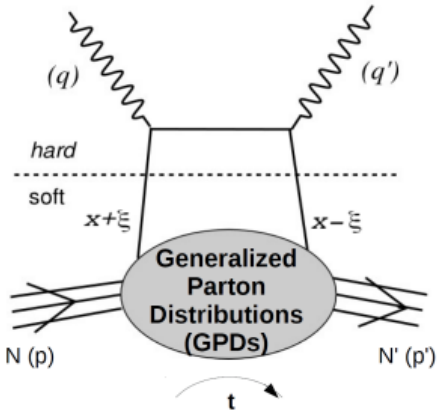

Fig. 3. The Feynman diagram for TCS, split into its hard and soft parts.[4]

1.2 Motivation:

Heavy meson production is a key tool for accessing the gluon GPDs of the proton. Muons are particles made of a quark q and its antiquark $\overline{q}$. Since the proton is made of up and down quarks (and strange quarks that can arise from the gluon sea), lighter muons such as $u\overline{u}$, $d\overline{d}$, and $s\overline{c}$ interact mostly with the valence and sea quarks in the proton, while heavier muons such as $c\overline{c}$ and $b\overline{b}$ interact mostly with the gluons. In fact, heavy mesons are the easiest particles to probe the gluon GPDs with, particularly the lightest form of $c\overline{c}$ (known as the J/ψ meson) and the lightest form of $b\overline{b}$ (known as Υ). For this reason, we will focus solely on the production of J/ψ and the three lightest stable resonances of Υ.

The hard exclusive production of J/ψ and Υ is dominated by two different reactions: one in which two gluons are exchanged and one where three are exchanged. It is thought that the three-gluon reaction dominates when there is barely enough energy to produce the meson, while the two-gluon reaction dominates at higher energies.[5]

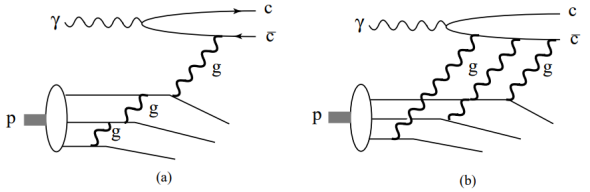

Fig. 4. The two- and three- gluon exchange methods of J/ψ production.[5]

Our goal with this experiment was to simulate the photoproduction, quasi-photoproduction, and electroproduction of the J/ψ and Υ mesons at a range of different energies and different proportions of the 2-gluon/3-gluon cross sections. These simulations can be used as a prediction of what might be observed at the upcoming Electron-Ion Collider (EIC), and will help guide the design of detectors in this collider to accurately measure these reactions. The ability to vary the proportion of the two- and three-gluon reactions will also help identify the proportion of the two reactions in experimental data.

2. Methods and Simulation

We implemented the simulations for the photoproduction, quasi-photoproduction, and electroproduction of $J\psi$ and Υ were as add-ons to the DEEPGen generator created by Marie Boer.[6] Due to the many similarities between the production of different mesons, we added a generic "meson production" reaction type. This type allows new meson production reactions to be added very easily and accounts for the common factors (such as virtual photon flux in electroproduction) present in all such reactions.

Each type of meson M is described by its mass distribution and one or more photoproduction differential cross-sections (i.e. probability density functions for the reaction $\gamma P \to MP$. Theoretically, the mass distributions for J/ψ and all Υ resonances should be relativistic Breit-Wigner distributions. However, since the width of these distributions is smaller than the resolution of most detectors, they are smeared into Gaussians. The peak of the Gaussian distribution for J/ψ is the consensus mass of $3.096\ GeV$,[7] with a customizable standard deviation. The peaks for the $1S, 2S, 3S$ resonances of Υ were taken to be $9.47, 10.01,$ and 10.36 respectively, with customizable deviations, and the normalization constants of these normal distributions were $22/40$, $11/40$, and $7/40$.[8]

For J/ψ production, the two-gluon and three-gluon differential cross sections[5] were

$$\frac{d\sigma_{(\gamma P \to J/\psi P, 2g)}}{dE_\gamma dQ'^2} = \frac{(1-y)^2}{(R_P\sqrt{Q'^2})^2} \tag{1}$$

$$\frac{d\sigma_{(\gamma P\to J/\psi P,3g)}}{dQ'^2} = \frac{1}{(R_P\sqrt{Q'^2})^4} \tag{2}$$

where R_P is the radius of the proton, E_γ is the energy of the incoming photon, Q'^2 is the virtuality of the outgoing photon and y is defined by

$$y := E_{\text{threshold}}/E_\gamma \tag{3}$$

We calculated E_{theshold} in the usual way to be $8.205\,GeV$ (see Appendix A).

For each simulation, we set the portion of two-gluon reactions a in an input file. Given this, the differential cross section used for photoproduction was

$$\frac{d\sigma_{(\gamma P\to MP)}}{dtdE_\gamma dQ'^2} = \frac{1}{16\pi}g(t)\left(a\frac{d\sigma_{(\gamma P\to J/\psi P,2g)}}{dE_\gamma dQ'^2} + (1-a)\frac{d\sigma_{(\gamma P\to J/\psi P,3g)}}{dQ'^2}\right) \tag{4}$$

$g(t)$ is the gluon form factor. This can be easily swapped to test different predicted form factors, but for simplicity was taken to be[5]

$$g(t) = e^{1.13t} \tag{5}$$

Only the 2-gluon cross section was implemented for Υ, due to a lack of theoretical development for the 3-gluon reaction. The 2-gluon cross-section was[9]

$$\frac{d\sigma_{(\gamma P\to \Upsilon P)}}{dxdt} = \frac{\pi}{4t^4}\left(\frac{4N_c^4}{(N_C^2-1)^2}G(x,t) + \sum_f |q_f(x,t)+\overline{q}_f(x,t)|\right)|F(t)|^2 \tag{6}$$

where t is the Mandelstam variable, x is the fraction of total proton momentum stored in each valence quark, $N_c = 3$ is the number of colors, $G(x,t)$ is the gluon GPD, $q_f(x,t)$ and $\overline{q}_f(x,t)$ are the GPDs for the quarks and antiquarks of flavor f, and $F(t)$ is the production amplitude. We used the Born production amplitude, which is given by

$$F(t) = C\frac{\alpha_s}{N_c}\frac{4\tau^2}{1-\tau^2}\ln\left(\frac{(1+\tau)^2}{4\tau}\right) \tag{7}$$

for $\tau = t/Q'^2$ and $C^2 = \frac{N_c\Gamma_{l^+l^-}Q'^3}{\alpha_{\text{em}}}$, with $\Gamma_{l^+l^-}$ being the lepton decay width of the meson.[9]

We used quark, antiquark, and gluon GPDs provided by the CTEQ project.[10] The most recent versions of these GPDs were used as of July 27th, 2021. For photoproduction, we used a factorization scale of $Q = 2\,GeV$.

The quasi-photoproduction reactions use the photoproduction cross sections in combination with a change of kinematic conditions, namely the use of bremsstrahlung

radiation as a source of photons instead of a pure photon beam. For electroproduction, the differential cross-sections are taken to be[11]

$$\frac{d\sigma_{(eP\to MP)}}{dtdQ'^2d\vec{A}} = \Phi(t,Q'^2)\frac{d\sigma_{(\gamma P\to MP)}}{d\vec{A}} \tag{8}$$

where $\vec{A}$ are the parameters of the normal photoproduction cross section and $\Phi(t,Q'^2)$ is the virtual photon flux factor given by[11]

$$\Phi(t,Q'^2) = \frac{\alpha_{\text{em}}}{2\pi Q^2(1+Q^2/M_P^2)^2}\left(\frac{1+(1-y)^2}{y} + \frac{2(1-y)}{7}\left(\frac{Q^2_{\text{min}}}{Q^2} - \frac{Q^2}{M_P^2}\right)\right) \tag{9}$$

where α_{em} is the electromagnetic coupling constant, Q^2 is the virtuality of the incoming photon, M_P is the proton mass, and $y = E_\gamma/E_{\text{el}}$ with E_{el} being the energy of the incoming electron.

The end product of the reaction is measured through its leptonic decay mode. Electron, muon, and pion decay can be chosen.

3. Results

DEEPGen produces a ROOT file containing several kinematic variables for each reaction. Most important among these are the virtuality of the outgoing photon Q' (which is equivalent to the mass of the meson produced) and the calculated differential cross section. Graphs of the cross section as a function of Q' are very close to what would be measured at a detector; thus these graphs were generated for a variety of conditions.

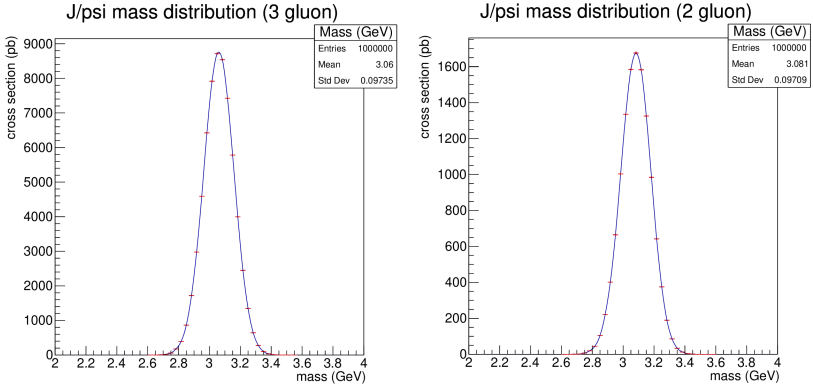

Fig. 5. Graphs of differential cross section (pb) vs. Q' for J/ψ photoproduction at low energy (5.5 - $11\ GeV$)

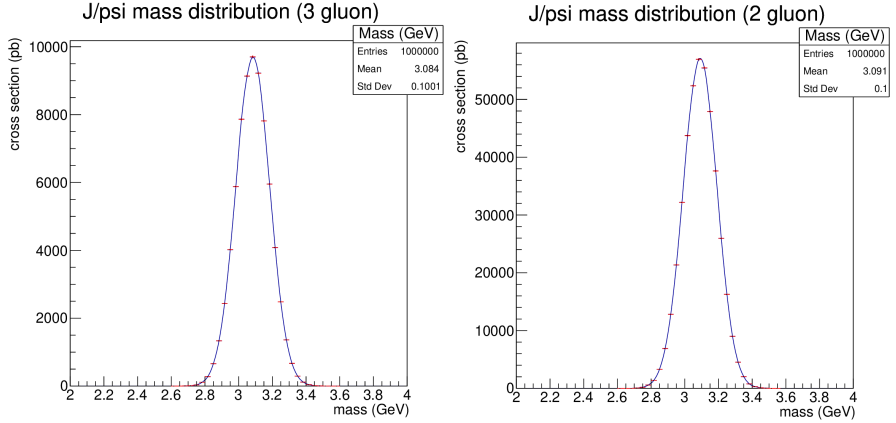

Fig. 6. Graphs of differential cross section (pb) vs. Q' for J/ψ photoproduction at high energy (100 - $200\,GeV$)

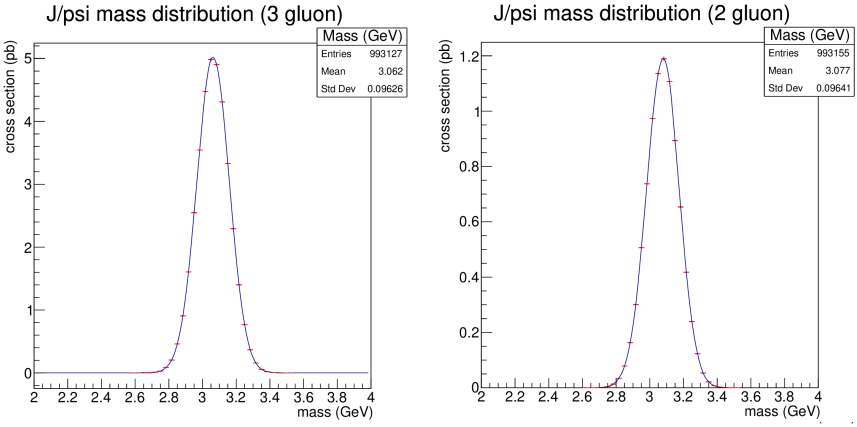

Fig. 7. Graphs of differential cross section (pb) vs. Q' for J/ψ electroproduction at low energy (5.5 - $11\,GeV$ photons, $11\,GeV$ electron beam)

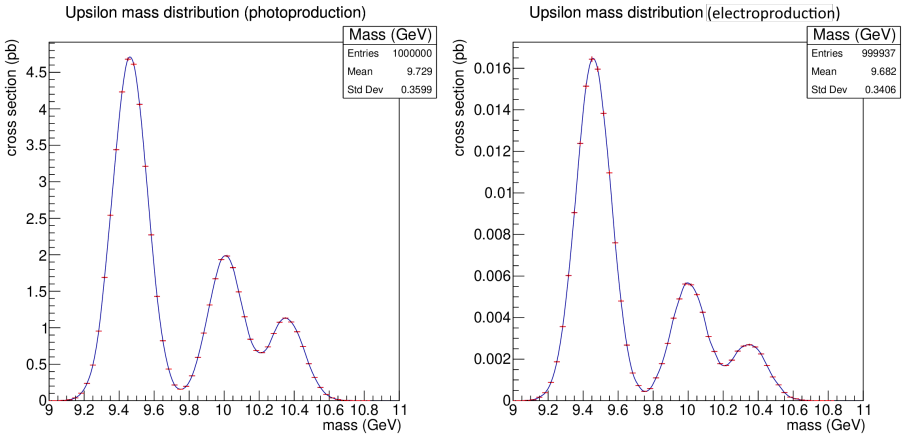

Fig. 8. Graphs of differential cross section (pb) vs. Q' for Υ photo- and electroproduction at high energy (100 - $200\ GeV$ photons, $41\ GeV$ electron beam)

4. Discussion

4.1 Two-gluon vs. three-gluon

It is worth noting that in the J/ψ production, the three-gluon cross section is significantly larger at lower energies, while the two-gluon cross section clearly dominates at higher energies. This is in line with theoretical predictions. At high energies, when the momentum of the created J/ψ can be large, the three-gluon mechanism is higher twist than the two-gluon mechanism, and is thus suppressed. Closer to threshold, however, the outgoing meson must be produced at a lower transverse momentum. This is difficult when only one quark interacts via a gluon with the meson, because the gluon must have a transverse momentum on at least the order of the mass of the produced quark to couple effectively to it. However, in the three-gluon exchange, the momentum of the three gluons interacting with the meson can cancel to almost nothing. This is reflected by the power of $(1-x)^2$ in the numerator of the two-gluon cross section, and thus in the graphs produced by the generator.[5] Thus the generator reflects the expected behavior of the two- and three-gluon cross sections at different energies.

4.2 Electroproduction

As expected, the cross-sections for electroproduction at a given energy is an order of 10^{-3} smaller than the cross-sections for photoproduction. This is as expected, as the cross-sections are related by a factor of $\alpha_{em} \approx 1/137$ representing the emission of a photon from the electron.

4.3 Bethe-Heitler background

One notable absence from this generator that would be present in experimental data is the Bethe-Heitler background. Since meson production is ultimately measured through the lepton pair the meson decays into, other processes which produce lepton pairs will always be a source of background. The dominant source of this is the Bethe-Heitler process, two dominant diagrams of which are pictured below:

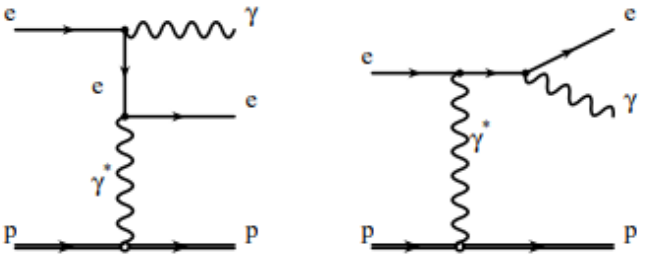

Fig. 9. Two dominant diagrams for the Bethe-Heitler process.[12] In this context, the produced photon would split into a lepton-antilepton pair which could be confused for the result of meson decay.

The choice to neglect this background was an intentional one, intended to allow us to focus exclusively on the meson production. Anyone wishing to use the generator as a reference or prediction for experimental data can simply add the generated events to a distribution of Bethe-Heitler events generated at the same energy (such Bethe-Heitler events can be generated from a wide array of generators, including DEEPSim).

4.4 High-energy photoproduction of J/ψ

It is worth noting that the cross sections calculated for J/ψ at high energies are extremely large. Without reference, it is unclear whether this will correspond to experimental data. However, there are two reasons to believe it may be inaccurate. The first is the extremely simple nature of the gluon form factors used. The second is that the differential cross-sections used were derived for production of J/ψ near threshold, and thus may not take into account behavior that arises at much higher energies. For reference, the Υ cross-section was repurposed with the decay widths of J/ψ to provide another calculation of the cross-sections at higher energies, and gave similar results. This may indicate that further theoretical work needs to be done on the production of J/ψ at higher energies.

5. Conclusion

Heavy meson production is an extremely powerful tool for accessing the gluon GPDs of the proton. We added a flexible framework for simulating hard exclusive meson production to the DEEPGen event generator and implemented cross sections for the J/ψ and $\Upsilon(1S, 2S, 3S)$ mesons. The generated events match well to experimental and theoretical predictions (aside from high energy J/ψ production, which was higher than expected). These simulations can be used to guide the design of detectors at the upcoming Electron-Ion Collider, as well as to provide a reference point for experimental data. By creating a flexible and accurate framework for simulating hard exclusive heavy meson production, we hope to guide upcoming experiments at the EIC and provide a valuable tool for future investigations into the nature of the proton.

Appendix A: Calculation of $E_{\text{threshold}}$ for J/ψ

The calculation of threshold energy for J/ψ production is based on two principles: the conservation of four-momentum magnitude, and the fact that when a particle is produced exactly at threshold, the particle in the center-of-mass frame is at rest.

Note that we will use natural units.

We consider the reaction $\gamma + P \to J/\psi + P$. In the lab frame, the proton is at rest, so we can write the four-momentum magnitude of the left side as

$$(\mathbf{p}_\gamma + \mathbf{p}_\mathbf{P})^2 = ((E_\gamma, 0, 0, E_\gamma) + (M_P, 0, 0, 0))^2 = (E_\gamma + M_P, 0, 0, E_\gamma)^2 \tag{10}$$

$$(\mathbf{p}_\gamma + \mathbf{p}_\mathbf{P})^2 = E_\gamma^2 + 2E_\gamma M_P + M_P^2 - E_\gamma^2 = 2E_\gamma M_P + M_P^2 \tag{11}$$

We then consider the four-momentum magnitude of the right side. In the center-of-mass frame, the J/ψ and the proton are considered as one particle with mass $M_{J/\psi} + M_P$; as previously mentioned, when the J/ψ is produced at threshold, this combined particle should be at rest. Thus the four-momentum magnitude of the right side should be

$$(M_{J/\psi} + M_P)^2 = M_{J/\psi}^2 + 2M_{J/\psi}M_P + M_P^2 \tag{12}$$

Setting the two four-momentum magnitudes equal to each other and solving for E_γ, we find that the E_γ at threshold is

$$E_{\text{threshold}} = \frac{M_{J/\psi}^2 + 2M_{J/\psi}M_P}{2M_P} \tag{13}$$

Using the consensus values of $M_{J/\psi} = 3.096\ GeV$ and $M_P = 0.938\ GeV$, we find that $E_{\text{threshold}} = 8.205\ GeV$.

Acknowledgements

Special thanks go out to Camillo Mariani, Betty Wilkins, and the staff at the Virginia Tech Neutrino REU for funding this research.

Tristan Anderson and Kevin Sanford both contributed valuable knowledge to this paper. Additionally, the paper could not have been completed without the invaluable logistical assistance of Jah'Shawn Ross.

References

1. Yan T-M, Drell S. The Parton Model and its Applications. International Journal of Modern Physics A, 2014;29(30): Available from: https://arxiv.org/abs/1409.0051. doi: 10.1142/S0217751X14300713.
2. CUSH, ed. Standard Model of Particle Physics + Gravity. Wikimedia Foundation, 2017; Available from: https://commons.wikimedia.org/wiki/File:Standard_Model_of_Elementary_Particles_%2B_Gravity.svg.
3. Brookhaven National Library, 2014; Available from: https://www.bnl.gov/today/body_pics/2014/11/gluonspin-hr.jpg.
4. Böer M. Deeply Virtual Compton Scattering and Generalized Parton Distributions. 2016;
5. Brodsky SJ, Chudakov A, Hoyer P, Laget JM. Photoproduction of charm near threshold. International Journal of Modern Physics B, 2001;498(1-2): Available from: https://arxiv.org/abs/hep-ph/0010343. doi: 10.1016/S0370-2693(00)01373-3.
6. Marie Boer, 2021; Available from: https://solid.jlab.org/wiki/index.php/DEEPGen_event_generator.
7. Nakamura, K et al, 2010; Available from: https://pdg.lbl.gov/2010/listings/rpp2010-list-J-psi-1S.pdf.
8. Collaboration C. Measurement of the Y(1S), Y(2S), and Y(3S) cross sections in pp collisions at sqrt(s) = 7 TeV. Physical Letters B, 2013;727. Available from: https://arxiv.org/abs/1303.5900. doi: 10.1016/j.physletb.2013.10.033.
9. Forshaw JR, Poludniowski G. Vector meson photoproduction at high-t and comparison to HERA data. European Physical Journal C, 2002;26. Available from: https://arxiv.org/abs/hep-ph/0107068. doi: 10.1140/epjc/s2002-01078-1.
10. CTEQ, 2021; Available from: https://ct.hepforge.org/.
11. Collaboration Z. Measurement of elastic ρ^0 photoproduction at HERA. Z. Phys C, 1995;69. Available from: https://arxiv.org/abs/hep-ex/9507011. doi: 10.1007/s002880050004.
12. Stamen R. Measurement of Deeply Virtual Compton Scattering at HERA. Thesis, 2001; Available from: https://core.ac.uk/download/pdf/25332597.pdf.